Strain effects and optical properties of $Si_{1-x}Ge_x/Si$ superlattices

Y. Rajakarunanayake and T. C. McGill
California Institute of Technology, Pasadena, California 91125

(Received 5 April 1989; accepted 14 April 1989)

We demonstrate that quasi direct band gap $Si_{1-x}Ge_x/Si$ superlattices can be obtained by suitable choices of layer thicknesses. We calculate strain dependent conduction-band offsets as functions of the substrate alloy concentration, and of the epilayer alloy concentration. Optical matrix elements are computed for $Si_{0.5}Ge_{0.5}/Si$ superlattices grown on $Si_{0.75}Ge_{0.25}$ buffer layers with superlattice layer thicknesses of 4 to 24 monolayers. We find that optical absorption and emission strengths can vary by three to four orders of magnitude for layer thickness variations as small as 1–2 monolayers, suggesting that layer thicknesses must be controlled to within one monolayer to obtain enhanced optical properties. Typical optical matrix elements calculated for these $Si_{1-x}Ge_x/Si$ superlattices are three to four orders of magnitude larger than for bulk Si or Ge, but, are still three orders of magnitude smaller than for direct band gap materials such as GaAs.

I. INTRODUCTION

Silicon and germanium have not been considered suitable materials for optoelectronic applications due to their indirect band gaps[1]; optical absorption strengths for pure Si and Ge are about six orders of magnitude lower than for a typical optoelectronic material such as GaAs.[2] However, recent advances in crystal-growth techniques, such as MBE (molecular-beam epitaxy), have made possible the fabrication of superlattices—layered epitaxial structures that possess electronic properties that are very different than those of their bulk constituents.[3] In particular, $Si_{1-x}Ge_x/Si$ superlattices grown on Si rich substrates seem to offer the intriguing possibility of greatly enhanced optical properties compared to pure Si or Ge.[4–12] A typical $Si_{1-x}Ge_x/Si$ superlattice grown in the [100] direction can be described as a crystal with energy bands folded into a reduced Brillouin zone. If the indirect conduction-band minimum in a material such as Si or Ge can be brought to the zone center Γ through the folding, the resulting band structure would be quasi direct.[9] In $Si_{1-x}Ge_x/Si$ superlattices grown in the z-direction, the folded X-conduction states are coupled to the top of the valence band by dipole matrix elements, for $\hat{x}$ and $\hat{y}$ polarizations. We have estimated that optical transition rates in these quasi direct $Si_{1-x}Ge_x/Si$ superlattices can be three to four orders of magnitude stronger than rates for phonon-assisted optical absorption in pure Si and Ge. A major issue of interest is whether such quasi direct $Si_{1-x}Ge_x/Si$ superlattices are promising candidates for optoelectronic devices.

The roles of strain, and of the valence-band offset in determining the alignments of the various bands in coherently strained $Si_{1-x}Ge_x/Si$ superlattices are discussed in Sec. II. In Sec. III we analyze a few illustrative $Si_{1-x}Ge_x/Si$ superlattices, and discuss the main features of their band structure. An interesting result we find for indirect superlattices is that, the lowest conduction band splits into a doublet due to an interference effect between the electrons from the two longitudinal valleys. We also derive a simple criterion for obtaining approximately quasi direct band structure,

$$k_{\min}^{Si} d^{Si} + k_{\min}^{Si_{1-x}Ge_x} d^{Si_{1-x}Ge_x} \approx 2n\pi + \delta. \quad (1)$$

Here, d^{Si} and $d^{Si_{1-x}Ge_x}$ are the layer thicknesses of the constituent layers, $k_{\min}^{Si}$ and $k_{\min}^{Si_{1-x}Ge_x}$ are the wave vectors of the longitudinal conduction valley minima, and δ is a small phase shift dependent on the particular band alignment. In Sec. IV we describe the calculation of optical properties using the envelope function approximation. We find that the optical absorption and emission strengths can vary by three to four orders of magnitude for layer thickness variations of 1–2 monolayers. Section V concludes the paper. A more detailed account of the calculation of the band structure of $Si_{1-x}Ge_x/Si$ superlattices is reported elsewhere.[13]

II. BAND OFFSET

Although the Si and Ge surfaces are chemically compatible, there is a lattice mismatch of $\approx 4.2\%$ between the two materials. Because of this mismatch, strain plays a crucial role in determining the relevant band alignments between these two materials. The heterojunction band offset for Si/Ge interfaces has been investigated by several groups. Kuech *et al.*[14] estimated the band discontinuities from reverse bias capacitance measurements, obtaining a valence-band offset of $E_V = 0.39 \pm 0.04$ eV. Margaritondo *et al*[15] report a valence-band offset of 0.2 eV based on photoemission studies; Mahowald *et al.*[16] obtain 0.4 ± 0.1 eV based on the same technique. The theoretical model of Harrison[17] gives a valence-band offset for Si/Ge of 0.38 eV. Tersoff[18] theory predicts a value of 0.18 eV, and more recent predictions of Harrison and Tersoff[19] set the valence-band offset at 0.29 eV. The above predictions can be in substantial error because there has been no provision for the effects of strain.

Recent *ab initio* density functional calculations by Van de Walle and Martin[20,21] have considered the effects of strain on the valence-band offsets explicitly. They find that the average positions of the valence-band edges of Si and Ge have an offset independent of strain ($\Delta E_V^{av} \approx 0.54 \pm 0.04$ eV). People and Bean[22,23] have been able to obtain remarkable agreement with several experimental results for the band-edge positions of Si/Ge structures by combining the valence-band offsets predicted by Van de Walle and Martin[20,21] with a phenomenological deformation potential the-

 © 1989 American Vacuum Society

ory. In this paper we have used a method similar to that of People and Bean[22,23] to obtain the heterojunction band alignments. Although there is still controversy about the value of the valence-band offset between Si and Ge, we expect the main results discussed in this paper to be qualitatively independent of the value of the valence-band offset.

The effects of the strain on a threefold degenerate Γ state can easily be included using the deformation potentials a, b, and d as discussed by Bir and Pikus.[24] We have taken the deformation potential parameters for Si and Ge from Balslev.[25] In our calculations, we have described the uniaxial splitting of the valence-band edge using the method of Hesagawa.[26] The effects of strain on the indirect conduction-band minima can be separated into a uniaxial splitting and a hydrostatic shift with respect to the unstrained position of the valence-band edge.[27] According to the calculations of Van de Walle and Martin,[20,21] the hydrostatic deformation component of the valence-band offset is quite small.

To assign the band alignments for quasi direct $Si_{1-x}Ge_x/Si$ superlattices, it is necessary to calculate the positions of the strain split conduction-band offsets. In particular, strain distribution in the epilayers will depend on whether the layers are thin enough to be coherently strained to the in-plane lattice constant of the buffer layer, or whether they will relax to the free standing superlattice configuration. In this paper we have assumed that the epitaxial layers are coherently strained to the in-plane lattice constant set by the buffer layer. However, this assumption is strictly valid only for epitaxial layers whose thicknesses do not exceed the critical thickness for pseudomorphic growth. For the ($\approx 4.2\%$) lattice mismatch between Si and Ge, the critical thickness is $\sim$20–30 Å.

For coherently strained superlattices, the conduction-band alignment will depend on the alloy concentration of the substrate, and on the alloy concentration in the epilayer. In Figs. 1 and 2, we show calculated conduction-band offsets for pseudomorphic growth of strained $Si_{1-x}Ge_x$ epitaxial layers on cubic $Si_{1-y}Ge_y$ substrates. The contour plot in

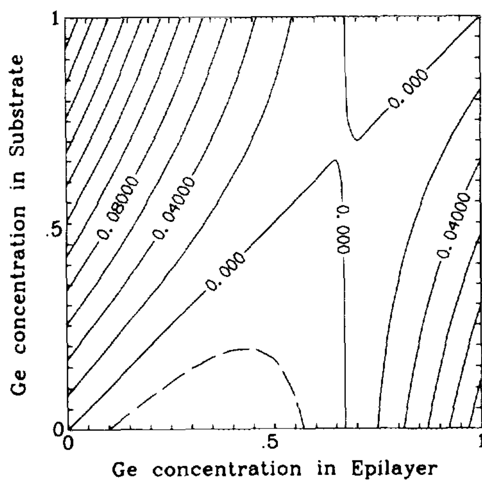

FIG. 1. The four-fold conduction-band offset (eV) (lattice matched to buffer) of a strained $Si_{1-x}Ge_x$ epitaxial layer grown pseudomorphically on an unstrained $Si_{1-y}Ge_y$ buffer layer. The conduction-band offset is measured with respect to the conduction-band position of the buffer layer.

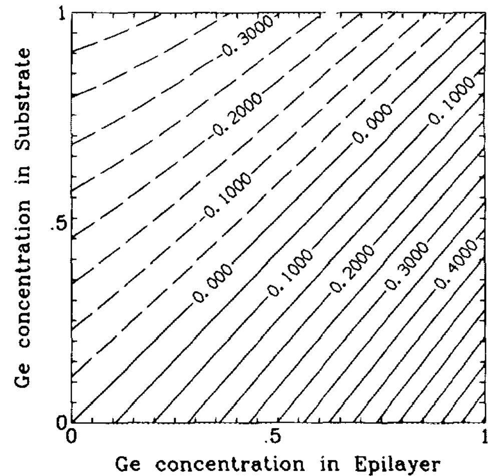

FIG. 2. The two-fold conduction-band offset (eV) (lattice matched to buffer) of a strained $Si_{1-x}Ge_x$ epitaxial layer grown pseudomorphically on an unstrained $Si_{1-y}Ge_y$ buffer layer. The conduction-band offset is measured with respect to the conduction-band position of the buffer layer.

Fig. 1 shows the conduction-band offset for the four-fold conduction minima relative to the unstrained conduction-band minimum of the substrate. The four-fold band offsets are relatively small (typically less than 100 meV) for most compositions. In Fig. 2 we show the band alignment of the twofold conduction bands relative to the unstrained conduction-band edge of the substrate; the two-fold band offsets can be considerably larger than the four-fold offsets (up to $\approx \pm 500$ meV). The values shown for the conduction-band offsets are applicable only for the movement of the X-valleys of $Si_{1-x}Ge_x$ alloys with strain. The L-point minima also have a characteristic splitting and a dependence on the alloy composition; these minima are the lowest conduction valleys in alloys with Ge concentrations in excess of $\approx 85\%$.

III. BAND STRUCTURE

The band structure of the lowest conduction band in a $Si_{0.5}Ge_{0.5}/Si$ superlattice was calculated using the four bulk states corresponding to $\pm k_{min} \pm \Delta k$; k_{min} is the position of the indirect minimum of the longitudinal conduction band. The most significant feature of the conduction band in indirect superlattices is that, due to the presence of the two longitudinal indirect valleys, the number of allowed solutions is doubled compared to the conduction band of a direct superlattice such as $GaAs$–$Al_xGa_{1-x}As$ ($x \leqslant 0.3$). Because of the interference between the electrons from the two longitudinal valleys, this additional degeneracy will be split. The actual splitting due to the interference effect is quite small (typically < 10 meV), and is a sensitive function of the layer thicknesses and the details of the matching conditions used; envelope function calculations give smaller interference effects than tight-binding calculations.[28] This interference effect in multivalley quantum well structures has been studied by many investigators.[28–30] Our predictions on the interference effect in $Si_{1-x}Ge_x/Si$ are in qualitative agreement with the work of Chang and Ting.[28]

We have picked a $Si_{0.5}Ge_{0.5}/Si$ superlattice grown on a $Si_{0.75}Ge_{0.25}$ layer to illustrate our analysis of $Si_{1-x}Ge_x/Si$

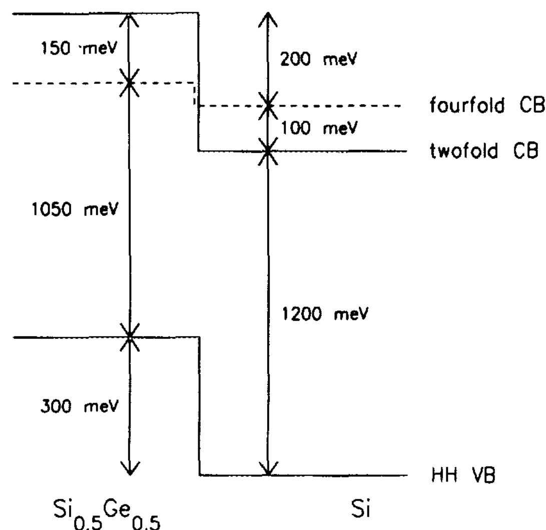

FIG. 3. Schematic diagram of the $Si_{0.5}Ge_{0.5}$ heterojunction band alignment indicating the relative positions of the two-fold, four-fold conduction bands and the heavy-hole valence bands. Strain distribution is calculated for pseudomorphic growth on a $Si_{0.75}Ge_{0.25}$ buffer layer. These band alignments are based on the valence-band offset of Van de Walle and Martin. The conduction-band offset seen by the electrons belonging to the two-fold valleys is 300 meV. The valence-band offset seen by the heavy holes is also 300 meV.

superlattices. In Fig. 3, we have shown the band alignment in the $Si_{0.5}Ge_{0.5}$/Si superlattice. The positions of the strain split conduction-band (CB) edges are shown as the two-fold and the four-fold CBs. The two-fold bands are the longitudinal valleys ($k_{\parallel} = 0$) with large effective masses along the growth direction. The four-fold bands are the transverse ellipsoids ($k_{\parallel} \neq 0$) in the x–y plane. The well material for the conduction band of the superlattice is Si. In Si layers grown on buffer layers with a larger in-plane lattice constant, the two-fold minima lie below the four-fold minima. In the barrier material, $Si_{0.5}Ge_{0.5}$ this situation is reversed.

We expect no coupling between the two-fold and the four-fold valleys since $k_{\parallel}$ is conserved across the interface. Thus, the barrier for the two-fold states in Si due to the $Si_{1-x}Ge_x$ layers is ≈ 300 meV, although the lowest conduction state in the barrier is the four-fold minimum that is only a 150 meV above the Si two-fold states. The large longitudinal mass of the two-fold band confines the superlattice states to typically < 100 meV above the bulk band edge. The four-fold states have smaller effective masses, and the superlattice states lie below the four-fold band edge in strained Si. Thus, we can neglect the presence of the folded four-fold minima since they correspond to higher conduction states. Furthermore, one does not expect optical transitions from the four-fold minima since their $k_{\parallel}$ component does not get zone folded to the Γ point.

In a typical situation, the band structure of the $Si_{0.5}Ge_{0.5}$/Si superlattice is expected to be indirect. For superlattices to be quasi direct, a special condition on the layer thicknesses must be satisfied. To a crude approximation, we can derive the condition for a superlattice to be quasi direct, by considering the conduction-band wave function of a $Si_{1-x}Ge_x$/Si superlattice to consist of a slowly varying envelope function of the Kronig Penny form, multiplied by a rapidly varying carrier wave that oscillates at k^{Si}_{min} or $k^{Si_{1-x}Ge_x}_{min}$ in the Si or $Si_{1-x}Ge_x$ layer respectively. For a superlattice to be quasi direct, the phase of the carrier wave should be close to a multiple of 2π; more precisely, the phase of the carrier wave should cancel the phase of the envelope function at the end of a superlattice period. The condition necessary for this phase cancellation is given in Eq. (1).

The superlattice band structure can change significantly even for small changes in layer thicknesses, as illustrated in Figs. 4(a), 4(b), and 4(c). Varying the layer thicknesses by only 1–2 monolayers (ML) causes the superlattice band structure to change from a direct configuration in 4(a), to an indirect configuration where the lowest point of the conduction band is pinned at the Brillouin zone edge, in 4(c). The superlattices shown in Fig. 4 are grown along the [001] direction, an $n \times m$ superlattice designates a structure with n monolayers of Si, and m monolayers of $Si_{1-x}Ge_x$ within a

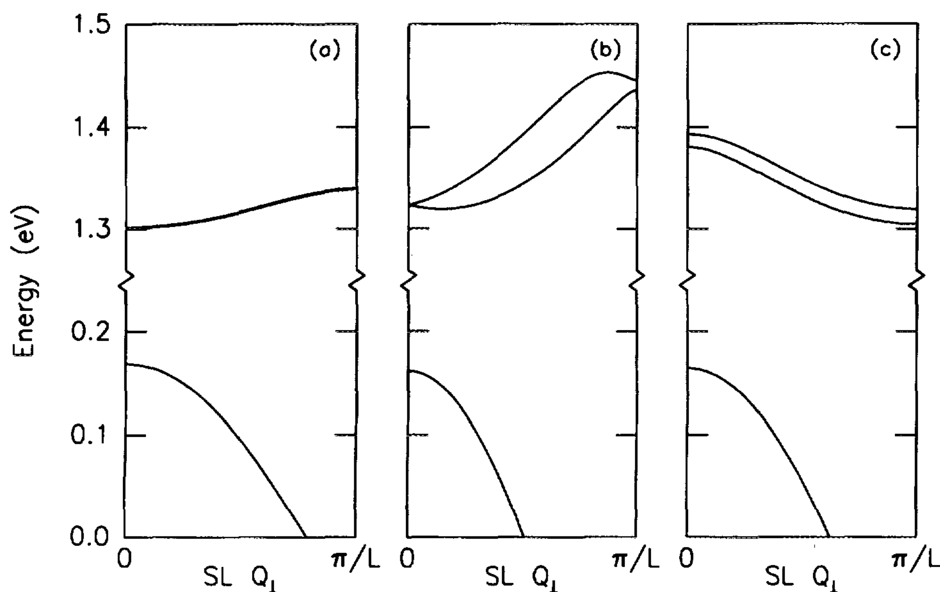

FIG. 4. Band structure of $Si_{0.5}Ge_{0.5}$/Si superlattices for three different layer thicknesses. The upper bands correspond to the longitudinal two-fold conduction bands, and the lower bands correspond to the heavy-hole bands. Here, $SLQ_{\perp}$ denotes the superlattice wave vector, and L is the period of the superlattice. Figure (a) shows a quasi direct band structure corresponding to a 7.2×7.2 monolayer superlattice. Figure (b) shows the indirect band structure of a 5×5 monolayer superlattice. Figure (c) shows the indirect band structure of a 6×6 superlattice in which the minimum of the conduction-band occurs at the edge of the reduced Brillouin zone.

single period. In Fig. 4(a) we have shown how a quasi direct superlattice can be achieved with a 7.2 ML×7.2 ML superlattice; since a 7×7 superlattice is only approximately quasi direct, we use fractional monolayers to achieve an illustrative quasi direct superlattice. In $Si_{1-x}Ge_x/Si$ superlattices with approximately equal layer thicknesses, the splitting of the lowest conduction-band doublet is quite small (almost degenerate). However, if the barrier and the well have different thicknesses, then the interference effect splits the almost degenerate conduction band into a doublet slightly separated in energy. Figure 4(b) is the band structure of a 5×5 $Si_{1-x}Ge_x/Si$ superlattice. The splitting of the lowest conduction band into a doublet is clearly shown. For a direct material with the same effective mass, the corresponding superlattice band structure would be a single conduction band at the average position of the lowest two conduction bands shown. In this case, the minimum of the superlattice conduction band lies at an arbitrary point along the folded Δ-axis. In Fig. 4(c) we show a 6×6 superlattice which has the conduction-band minimum at the reduced zone boundary. In all three sections of Fig. 4, we have shown the band structure of the heavy-hole state. In contrast to the behavior of the conduction band, the valence band does not exhibit a significant variation for small changes in the layer thicknesses. We find that, in order to achieve a given band structure, it is important to control the layer thicknesses to roughly within 1 ML.

IV. OPTICAL PROPERTIES

While a direct band gap is necessary for good optical emission, it is not sufficient. We also need a finite value for the optical matrix element. The optical absorption and emission strengths are proportional to the square of the momentum matrix element between the conduction and the valence bands. In $Si_{1-x}Ge_x/Si$, the conduction-band wave function is composed of a rapidly varying carrier wave multiplied by a slowly varying envelope function that mimics a conventional Kronig Penney solution, while the valence-band wave function has only a slowly varying envelope function. Although transitions between the first conduction band and the top of the valence band are dipole allowed, the coupling between these states through the momentum matrix element is quite small since the conduction and valence wave functions have different Fourier components and are nearly orthogonal, in spite of the band folding. Thus, in a typical situation, the superlattice optical matrix element M_{op}^{SL} is small (10^{-5}–10^{-2} atomic units); in comparison to the square of the optical matrix element for bulk GaAs, $|M_{op}|^2 \simeq 1.86$ (atomic units),[31] the direct absorption strengths of $Si_{1-x}Ge_x/Si$ superlattices are three–four orders of magnitude smaller.

In Fig. 5 we show the square of the optical matrix element versus the layer thicknesses for the transition from the lowest conduction-band state to the corresponding valence-band state. The expected matrix elements are quite small, as explained in the previous section, with the major contribution to the optical matrix element integral coming from the interfaces. Thus, the phase of the conduction-band wave function at each interface plays an important role in determining the optical matrix element. Because of this phase dependence at the interface, the optical matrix element in

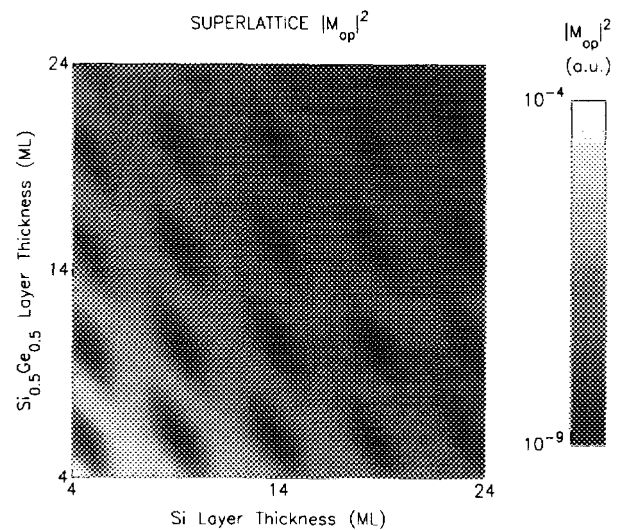

FIG. 5. Grey scale plot of $|M_{op}|^2$ (square of the optical matrix element) as a function of the layer thicknesses of Si and $Si_{0.5}Ge_{0.5}$ within a single period of the superlattice. $|M_{op}|^2$ is in atomic units; for comparison, in bulk GaAs $|M_{op}|^2 = 1.86$. The darker regions correspond to superlattices with enhanced optical matrix elements. Note that layer thickness variations of 1–2 ML can change the optical matrix elements by three–four orders of magnitude.

$Si_{1-x}Ge_x/Si$ superlattices is a very sensitive function of the layer thicknesses. As can be seen in Fig. 5, changing the thickness of either layer by approximately 2–3 ML (corresponding to a phase change of π), can change the absorption and emission strengths by several orders of magnitude. The largest optical matrix elements occur at small layer thicknesses, where a large interface-to-volume ratio exists. As the layer thicknesses are increased, the optical matrix elements decrease because the interface to volume ratio in the superlattice decreases. In the parameter space of 4–24 ML, the maximum optical matrix elements occur near the 6×8 $Si_{1-x}Ge_x/Si$ superlattice.

V. CONCLUSIONS

We have calculated the band structure and optical properties of $Si_{1-x}Ge_x/Si$ superlattices using the envelope function apporoximation. We have shown how the band structure of indirect superlattices such a $Si_{1-x}Ge_x/Si$ can be tailored to obtain approximately quasi direct band gaps by following a simple prescription given by Eq. (1). The optical matrix elements associated with these new quasi direct transitions can be three to four orders of magnitude larger than the phonon assisted absorption strengths in pure Si or Ge. However, the band folded states yield much weaker optical matrix elements that are still approximately three orders of magnitude smaller than those in bulk materials with direct band gaps such as GaAs. Finally we observe that it is necessary to control the layer thicknesses to within a single monolayer in order to achieve the enhanced optical absorption and emission.

ACKNOWLEDGMENTS

This work was supported by the Defense Advanced Projects Agency under Contract No. N00014-K-86-0841. We

would also like to acknowledge useful discussions with E. T. Yu, R. H. Miles, and R. J. Hauenstein.

[1]K. E. Peterson, Proc. IEEE **70**, 420 (1982).
[2]S. M. Sze, *Physics of Semiconductor Devices* (Wiley, New York, 1981).
[3]L. Esaki and R. Tsu, IBM. J. Res. Dev. **40**, 61 (1970).
[4]R. Hull, J. M. Gibson, and J. C. Bean, Appl. Phys. Lett. **46**, 179 (1985).
[5]R. People, J. C. Bean, D. V. Lang, A. M. Sergent, H. L. Stormer, K. W. Wecht, R. T. Lynch, and K. Baldwin, Appl. Phys. Lett. **45**, 1231 (1984).
[6]J. C. Bean, L. C. Feldman, A. T. Fiory, S. Nakahara, and I. K. Robinson, J. Vac. Sci. Technol. A **2**, 434 (1984).
[7]H. M. Manasevit, I. S. Gergis, and A. B. Jones, Appl. Phys. Lett. **41**, 464 (1982).
[8]E. Kasper and J. C. Bean, *Silicon Molecular Beam Epitaxy* (Chemical Rubber, Boca Raton, 1987).
[9]S. A. Jackson and R. People, Mater. Res. Soc. Symp. Proc. **56**, 365 (1986).
[10]J. C. Bean, Mater. Res. Soc. Symp. Proc. **37**, 245 (1985).
[11]S. Froyen, D. M. Wood, and A. Zunger, Phys. Rev. B **37**, 6893 (1988).
[12]M. S. Hybertsen and M. Schluter, Phys. Rev. B **36**, 9683 (1987).
[13]Y. Rajakarunanayake and T. C. McGill, Phys. Rev. B (to be published).
[14]T. F. Keuch, M. Mäenpää, and S. S. Lau, Appl. Phys. Lett. **39**, 245 (1981).
[15]G. Margaritondo, A. D. Katnani, N. G. Stoffel, R. R. Daniels, and T. X. Zhao, Solid State Commun. **43**, 163 (1982).
[16]P. H. Mahowald, R. S. List, W. E. Spicer, and P. Pianetta, J. Vac. Sci. Technol. B **3**, 1252 (1985).
[17]W. A. Harrison, *Electronic Structure and Properties of Solids* (Freeman, San Francisco, 1980).
[18]J. Tersoff, Phys. Rev. B **30**, 4874 (1984).
[19]W. A. Harrison and J. Tersoff, J. Vac. Sci. Technol. B **4**, 1068 (1986).
[20]C. G. Van de Walle and R. M. Martin, J. Vac. Sci. Technol. B **3**, 1256 (1985).
[21]C. G. Van de Walle and R. M. Martin, Phys. Rev. B **34**, 5621 (1986).
[22]R. People, Phys. Rev. B **32**, 1405 (1985).
[23]R. People and J. C. Bean, Appl. Phys. Lett. **48**, 538 (1986).
[24]G. L. Bir and G. E. Pikus, *Symmetry and Strain Induced Effects in Semiconductors* (Keter, Jerusalem, 1974).
[25]I. Balslev, Phys. Rev. **143**, 636 (1966).
[26]H. Hesagawa, Phys. Rev. **129**, 1029 (1962).
[27]J. C. Hensel and G. Feher, Phys. Rev. **129**, 1041 (1963).
[28]Y. C. Chang and D. Z. Ting, J. Vac. Sci. Technol. B **1**, 435 (1983).
[29]M. Nakayama and L. J. Sham, Solid State Commun. **26**, 6 (1978).
[30]L. J. Sham and M. Nakayama, Surf. Sci. **73**, 272 (1978); Phys. Rev. B **20**, 734 (1979).
[31]C. W. Higginbotham, Ph.D. thesis, Brown University, 1970.